Ergod. Th. & Dynam. Sys., (2022), **42**, 389–401 © The Author(s), 2021. Published by Cambridge University Press.
doi:10.1017/etds.2021.14

Flexibility of measure-theoretic entropy of boundary maps associated to Fuchsian groups

ADAM ABRAMS†, SVETLANA KATOK‡ and ILIE UGARCOVICI§

† *Institute of Mathematics, Polish Academy of Sciences, Warsaw 00656, Poland*
(e-mail: the.adam.abrams@gmail.com)
‡ *Department of Mathematics, The Pennsylvania State University, University Park, PA 16802, USA*
(e-mail: sxk37@psu.edu)
§ *Department of Mathematical Sciences, DePaul University, Chicago, IL 60614, USA*
(e-mail: iugarcov@depaul.edu)

(*Received* 14 *September* 2019 *and accepted in revised form* 15 *June* 2020)

In memory of Tolya

Abstract. Given a closed, orientable, compact surface S of constant negative curvature and genus $g \geq 2$, we study the measure-theoretic entropy of the Bowen–Series boundary map with respect to its smooth invariant measure. We obtain an explicit formula for the entropy that only depends on the perimeter of the $(8g-4)$-sided fundamental polygon of the surface S and its genus. Using this, we analyze how the entropy changes in the Teichmüller space of S and prove the following flexibility result: the measure-theoretic entropy takes all values between 0 and a maximum that is achieved on the surface that admits a regular $(8g-4)$-sided fundamental polygon. We also compare the measure-theoretic entropy to the topological entropy of these maps and show that the smooth invariant measure is not a measure of maximal entropy.

Key words: Fuchsian groups, boundary maps, entropy, Teichmüller space
2020 Mathematics Subject Classification: 37D40, 37E10 (Primary); 28D20, 20H10 (Secondary)

1. *Introduction*

Any closed, orientable, compact surface S of genus $g \geq 2$ and constant negative curvature can be modeled as $S = \Gamma\backslash\mathbb{D}$, where $\mathbb{D} = \{z \in \mathbb{C} : |z| < 1\}$ is the unit disk endowed with hyperbolic metric

$$\frac{2|dz|}{1-|z|^2} \tag{1}$$

and Γ is a finitely generated Fuchsian group of the first kind acting freely on $\mathbb{D}$.

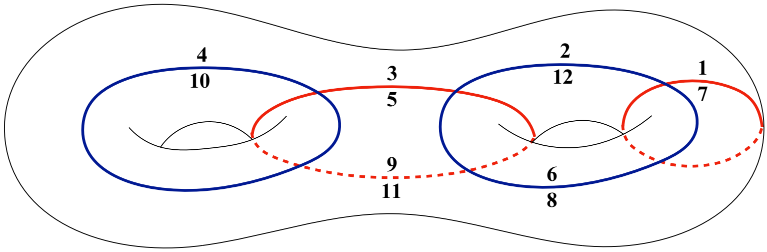

FIGURE 1. Chain of $2g$ geodesics when $g = 2$.

Recall that geodesics in this model are half-circles or diameters orthogonal to $\mathbb{S} = \partial\mathbb{D}$, the circle at infinity. The geodesic flow $\widetilde{\varphi}^t$ on $\mathbb{D}$ is defined as an $\mathbb{R}$-action on the unit tangent bundle $T^1\mathbb{D}$ that moves a tangent vector along the geodesic defined by this vector with unit speed. The geodesic flow $\widetilde{\varphi}^t$ on $\mathbb{D}$ descends to the geodesic flow φ^t on the factor $S = \Gamma\backslash\mathbb{D}$ via the canonical projection

$$\pi : T^1\mathbb{D} \to T^1 S$$

of the unit tangent bundles. The orbits of the geodesic flow φ^t are oriented geodesics on S.

A surface S of genus g admits an $(8g-4)$-sided fundamental polygon $\mathcal{F}$ obtained by cutting it with $2g$ closed geodesics that intersect in pairs (g of them go around the 'holes' and another g go around the 'waists' of S) (see Figure 1).

The existence of such a fundamental polygon $\mathcal{F}$ is an old result attributed [4, 19] to Dehn, Fenchel, Nielsen, and Koebe. Adler and Flatto [3, Appendix A] give a careful proof of existence and properties of $\mathcal{F}$.

We label the sides of $\mathcal{F}$ in a counterclockwise order by numbers $1 \le i \le 8g-4$ and label the vertices of $\mathcal{F}$ by V_i so that side i connects V_i to $V_{i+1} \pmod{8g-4}$ (this gives us a *marking* of the polygon).

We denote by P_i and Q_{i+1} the endpoints of the oriented infinite geodesic that extends side i to the circle at infinity $\mathbb{S}$. (The points P_i, Q_i in this paper and [1, 2, 6, 12] are denoted by a_i, b_{i-1}, respectively, in [3].) The order of endpoints on $\mathbb{S}$ is the following:

$$P_1, Q_1, P_2, Q_2, \ldots, P_{8g-4}, Q_{8g-4}.$$

The identification of the sides of $\mathcal{F}$ is given by the side pairing rule

$$\sigma(i) := \begin{cases} 4g - i \bmod (8g-4) & \text{if } i \text{ is odd,} \\ 2 - i \bmod (8g-4) & \text{if } i \text{ is even.} \end{cases} \tag{2}$$

Let T_i denote the Möbius transformation pairing side i with side $\sigma(i)$.

Notice that in general the polygon $\mathcal{F}$, whose sides are geodesic segments, need not be regular, but the sides i and $\sigma(i)$ must have equal length and the angles at vertices i and $\sigma(i)+1$ must add up to π. The last property implies the 'extension condition', which is crucial for our analysis: the extensions of the sides of $\mathcal{F}$ do not intersect the interior of the tessellation $\gamma\mathcal{F}$, $\gamma \in \Gamma$ (see Figure 2). If $\mathcal{F}$ is regular (see [3, Figure 1]), it is the Ford fundamental domain, that is, P_iQ_{i+1} is the isometric circle for T_i, and $T_i(P_iQ_{i+1}) = Q_{\sigma(i)+1}P_{\sigma(i)}$ is the isometric circle for $T_{\sigma(i)}$, so that the inside of the former

https://doi.org/10.1017/etds.2021.14 Published online by Cambridge University Press

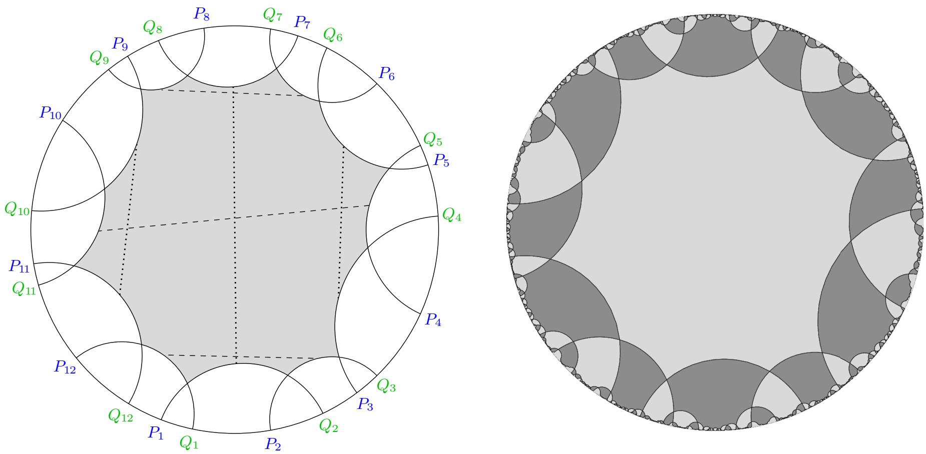

FIGURE 2. An irregular polygon with side identifications (left) and tessellation (right), genus 2.

isometric circle is mapped to the outside of the latter, and all internal angles of $\mathcal{F}$ are equal to $\pi/2$.

For each fundamental polygon $\mathcal{F}$ with sides along geodesics $P_i Q_{i+1}$, the *Bowen–Series boundary map* $f_{\bar{P}} : \mathbb{S} \to \mathbb{S}$ is defined as

$$f_{\bar{P}}(x) = T_i x \quad \text{if } x \in [P_i, P_{i+1}). \tag{3}$$

The map admits a unique smooth ergodic invariant measure $\mu_{\bar{P}}$ (see [6, Theorem 1.2]). Adler and Flatto [3] gave a thorough analysis of these maps, their two-dimensional natural extensions, and applications to the symbolic coding of the geodesic flow on $\Gamma\backslash\mathbb{D}$. They also describe the measure $\mu_{\bar{P}}$ as a two-step projection of the invariant Liouville measure for the geodesic flow.

We can now state our first main result.

THEOREM 1. *The entropy of the boundary map with respect to its smooth invariant measure is given by*

$$h_{\mu_{\bar{P}}}(f_{\bar{P}}) = \frac{\pi^2(4g-4)}{\text{Perimeter}(\mathcal{F})} = \pi \cdot \frac{\text{Area}(\mathcal{F})}{\text{Perimeter}(\mathcal{F})}. \tag{4}$$

Let $S = \Gamma\backslash\mathbb{D}$ be any compact surface of genus $g \geq 2$ and $S_0 = \Gamma_{\text{reg}}\backslash\mathbb{D}$ be a special genus g surface that admits a regular $(8g-4)$-sided fundamental region $\mathcal{F}_{\text{reg}}$. By the Fenchel–Nielsen theorem there exists an orientation-preserving homeomorphism h from $\bar{\mathbb{D}}$ onto $\bar{\mathbb{D}}$ such that $\Gamma = h \circ \Gamma_{\text{reg}} \circ h^{-1}$ and the sides of the fundamental polygon $\mathcal{F}$ for Γ belong to geodesics $P_i' Q_{i+1}'$, where $P_i' = h(P_i)$, $Q_{i+1}' = h(Q_{i+1})$ and $P_i Q_{i+1}$ are the extensions of the sides of $\mathcal{F}_{\text{reg}}$. The map $h|_{\mathbb{S}}$ is a homeomorphism of $\mathbb{S}$ preserving the order of the points $\{P_i\} \cup \{Q_i\}$.

The Teichmüller space $\mathcal{T}(S)$ of a surface S can be thought of as any of the following:

(i) the space of Riemann surface structures on S modulo conformal maps isotopic to the identity [8, §1];

(ii) the space of marked Fuchsian groups Γ such that $\pi_1(S) \xrightarrow{\sim} \Gamma$ and S is orientation-preserving homeomorphic to $\Gamma\backslash\mathbb{D}$ [9, Definition 2.1.1];

(iii) the space of all marked canonical hyperbolic $(8g-4)$-gons in the unit disk $\mathbb{D}$ such that side i and side $\sigma(i)$ have equal length and the internal angles at vertices i and $\sigma(i)+1$ sum to π, up to an isometry of $\mathbb{D}$. (The topology on the space of polygons is $\mathcal{P}_k \to \mathcal{P}$ if and only if the lengths of all sides converge and the measures of all angles converge.)

The space $\mathcal{T}(S)$ is homeomorphic to $\mathbb{R}^{6g-6}$. A standard way to parametrize $\mathcal{T}(S)$ is through Fenchel–Nielsen coordinates (see the classical manuscript recently published in [7]). The surface S can be decomposed along $3g-3$ simple closed curves into $2g-2$ pairs of pants (shown for $g=3$ at the bottom of Figure 4). For any $S' \in \mathcal{T}(S)$, these curves are canonically represented by geodesics, whose lengths determine each pair of pants up to isometry. To recover S' we need in addition twist parameters when gluing pants together. Thus altogether $\mathcal{T}(S)$ is parametrized by $\mathbb{R}_+^{3g-3} \times \mathbb{R}^{3g-3}$ (the first group of parameters are called the *lengths* and the second the *twists*), and $\dim \mathcal{T}(S) = 6g-6$.

The construction (iii) of $\mathcal{T}(S)$ by varying 'marked' fundamental polygons is less common than the others. Following the earlier work [18, 20], Schmutz Schaller [16] considers canonical $4g$-gons, but the canonical $(8g-4)$-gons may be considered as well. The following is a heuristic argument for the derivation of the dimension of $\mathcal{T}(S)$ using the $(8g-4)$-gon: the lengths of the identified pairs of sides are given by $4g-2$ real parameters; $2g-1$ real parameters represent the angles since four angles at each vertex are determined by one real parameter. The dimension of the space of isometries of $\mathbb{D}$ is 3, so we remain with $(4g-2)+(2g-1)-3 = 6g-6$ parameters.

A few years ago, Anatole Katok suggested a new area of research—or, at the very least, a new viewpoint—called the 'flexibility program', which can be broadly formulated as follows: under properly understood general restrictions, within a fixed class of smooth dynamical systems some dynamical invariants take arbitrary values. Taking this point of view, it is natural to ask how the measure-theoretic entropy $h_{\mu_{\bar{P}}}(f_{\bar{P}})$ changes in $\mathcal{T}(S)$. Our second main result addresses this question.

THEOREM 2. (Maximum and flexibility of entropy)

(i) *Among all surfaces in $\mathcal{T}(S)$, the maximum value of the entropy $h_{\mu_{\bar{P}}}(f_{\bar{P}})$ is achieved on the surface for which $\mathcal{F}$ is regular and is equal to*

$$H(g) := h_{\mu_{\bar{P}}^{\mathrm{reg}}}(f_{\bar{P}}^{\mathrm{reg}}) = \frac{\pi^2(4g-4)}{(8g-4)\cosh^{-1}(1+2\cos(\pi/(4g-2)))}. \tag{5}$$

(ii) *For any value $h \in (0, H(g)]$ there exists $\mathcal{F} \in \mathcal{T}(S)$ such that $h_{\mu_{\bar{P}}}(f_{\bar{P}}) = h$.*

This paper is organized as follows. In §2 we prove Theorem 1. The natural extension $F_{\bar{P}}$ of $f_{\bar{P}}$ and the 'geometric map' F_{geo} from [1] are used in the proof. In §3 we prove Theorem 2 by invoking the isoareal inequality and using Fenchel–Nielsen coordinates in the Teichmüller space related to a fundamental $(8g-4)$-gon. In §4 we compare the topological entropy of the boundary map $f_{\bar{P}}$ to the measure-theoretic entropy and show that the smooth invariant measure $\mu_{\bar{P}}$ is not a measure of maximal entropy. In Appendix A we provide some computational tools for genus 2.

2. *Proof of Theorem 1*

The space of oriented geodesics on $\mathbb{D}$ is modeled as $\mathbb{S}\times\mathbb{S}\setminus\Delta$, where Δ is the diagonal $\{(w,w): w\in\mathbb{S}\}$. The smooth measure

$$d\nu=\frac{|du||dw|}{|u-w|^2}$$

on $\mathbb{S}\times\mathbb{S}\setminus\Delta$ was most probably first considered by Hopf [10] as he introduced the measure $dm=d\nu ds$ on $T^1(\mathbb{D})$ to study ergodic properties of the geodesic flow. The measure $d\nu$ was later used by Sullivan [17], Bonahon [5], Adler and Flatto [3], and the current authors [1, 12]. The measure dm is often more convenient for studying the geodesic flow than the Liouville volume

$$d\omega=\frac{4\,dx\,dy\,d\theta}{(1-x^2-y^2)^2},$$

which comes from the hyperbolic measure on $\mathbb{D}$. Both measures $d\nu$ and dm are preserved by Möbius transformations, and $d\omega=\frac{1}{2}dm$ (see [5, Appendix A2]). (The constant relating $d\omega$ and dm was given incorrectly as $1/4$ in [3, p. 250]. Following that, $1/4$ was used in [1, Proposition 10.1].)

Adler and Flatto [3] introduced the 'rectilinear map' defined by

$$F_{\bar{P}}(u,w)=(T_iu,T_iw)\quad\text{if } w\in[P_i,P_{i+1}) \tag{6}$$

and showed the existence of an invariant domain $\Omega_{\bar{P}}\subset\mathbb{S}\times\mathbb{S}$ such that $F_{\bar{P}}$ restricted to $\Omega_{\bar{P}}$ is a two-dimensional geometric realization of the natural extension map of $f_{\bar{P}}$. (In [12], the authors showed that $\Omega_{\bar{P}}$ is also the global attractor of $F_{\bar{P}}:\mathbb{S}\times\mathbb{S}\setminus\Delta\to\mathbb{S}\times\mathbb{S}\setminus\Delta$.) The set $\Omega_{\bar{P}}$ is bounded away from the diagonal Δ and has a finite rectangular structure. Thus $F_{\bar{P}}$ preserves the smooth probability measure

$$d\nu_{\bar{P}}:=\frac{d\nu}{\int_{\Omega_{\bar{P}}}d\nu}.$$

The boundary map $f_{\bar{P}}$ is a factor of $F_{\bar{P}}$ (projecting on the second coordinate), so one can obtain its smooth invariant probability measure $\mu_{\bar{P}}$ as a projection.

The geodesic flow on S can be realized as a special flow over a cross-section that is parametrized by $\Omega_{\bar{P}}$, and the first return map to this cross-section acts exactly as $F_{\bar{P}}:\Omega_{\bar{P}}\to\Omega_{\bar{P}}$. Using this realization along with Abramov's formula and the Ambrose–Kakutani theorem, we have from [1, Proposition 10.1] (with a corrected constant) that

$$h_{\mu_{\bar{P}}}(f_{\bar{P}})=h_{\nu_{\bar{P}}}(F_{\bar{P}})=\frac{\pi^2(4g-4)}{\int_{\Omega_{\bar{P}}}d\nu},$$

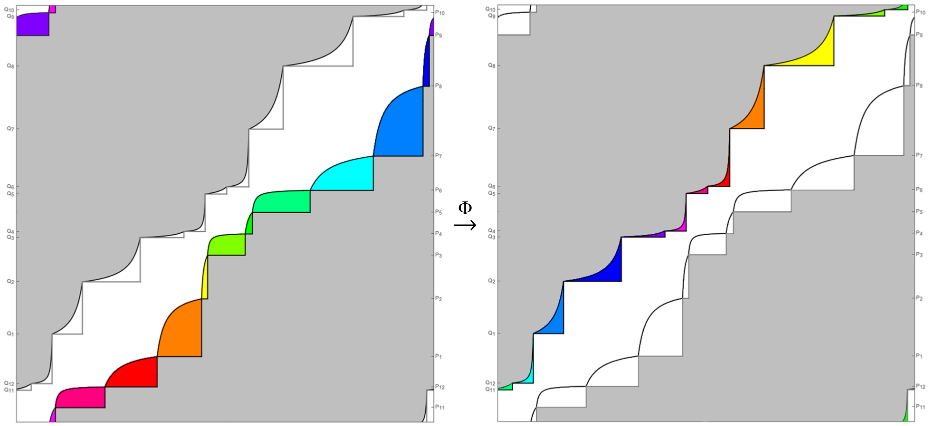

FIGURE 3. Bulges $\mathcal{B}_i$ of Ω_{geo} (left) are mapped to corners of $\Omega_{\bar{P}}$ (right).

and since $\text{Area}(\mathcal{F}) = 2\pi(2g-2)$ by the Gauss–Bonnet formula, we have

$$h_{\mu_{\bar{P}}}(f_{\bar{P}}) = \pi \cdot \frac{\text{Area}(\mathcal{F})}{\int_{\Omega_{\bar{P}}} d\nu}. \tag{7}$$

To prove Theorem 1, it remains only to show that $\int_{\Omega_{\bar{P}}} d\nu$ is equal to the (hyperbolic) perimeter of $\mathcal{F}$. For that, we use another map, also introduced by Adler and Flatto in [3], called the 'curvilinear map' (or 'geometric map' in [1]). Denoting by uw the geodesic from u to w, the map is defined on the set

$$\Omega_{\text{geo}} := \{(u, w) : uw \text{ intersects } \mathcal{F}\} \subset \mathbb{S} \times \mathbb{S} \setminus \Delta$$

and is given by

$$F_{\text{geo}}(u, w) = (T_i u, T_i w) \quad \text{if } uw \text{ exits } \mathcal{F} \text{ through side } i.$$

There is a key correspondence between Ω_{geo} and $\Omega_{\bar{P}}$ (see Figure 3).

PROPOSITION 3. [3, Theorem 5.1] *The map* $\Phi : \Omega_{\text{geo}} \to \Omega_{\bar{P}}$ *given by*

$$\Phi = \begin{cases} \text{Id} & \text{on } \Omega_{\text{geo}} \cap \Omega_{\bar{P}}, \\ T_{\sigma(i)-1} T_i & \text{on } \mathcal{B}_i, \end{cases}$$

where $\mathcal{B}_i = \{(u, w) \in \Omega_{\text{geo}} \setminus \Omega_{\bar{P}} : w \in [P_i, P_{i+1}]\}$, *is bijective.*

Since Φ acts by fractional linear transformations, which preserve the measure ν, we have that

$$\int_{\Omega_{\bar{P}}} d\nu = \int_{\Omega_{\text{geo}}} d\nu. \tag{8}$$

Having proved (8), we now want to show that $\int_{\Omega_{\text{geo}}} d\nu$ is equal to the (hyperbolic) perimeter of $\mathcal{F}$.

https://doi.org/10.1017/etds.2021.14 Published online by Cambridge University Press

LEMMA 4. (Bonahon) *For any oriented geodesic segment s on $\mathbb{D}$,*

$$\int_{\Psi^+(s)} d\nu = \text{length}(s),$$

where $\Psi^+(s)$ is the set of oriented geodesics intersecting s with the oriented angle at the intersection between 0 and π.

The proof involves expressing $d\nu = |du||dw|/|u-w|^2$ in a coordinate system (x, θ) based on movement along geodesics, namely,

$$d\nu = \tfrac{1}{2} \sin(\theta)\, d\theta\, dx,$$

where x is the distance along the segment s from the point of intersection of s with uw, and θ is the angle that uw makes with s. (This measure is sometimes called 'geodesic current'.) See [**5**, Appendix A3] for details†.

Recall that the domain Ω_{geo} of the geometric map F_{geo} consists of all (u, w) for which uw intersects $\mathcal{F}$. This can be decomposed as $\Omega_{\text{geo}} = \bigcup_{i=1}^{8g-4} \mathcal{G}_i$, where

$$\mathcal{G}_i = \{(u, w) : uw \text{ exits } \mathcal{F} \text{ through side } i\} = \Psi_+(\text{side } i)$$

(these 'strips' are shown in [**1**, Figure 3]). Thus from Lemma 4 we immediately get

$$\int_{\Omega_{\text{geo}}} d\nu = \sum_{i=1}^{8g-4} \int_{\mathcal{G}_i} d\nu = \sum_{i=1}^{8g-4} \text{length}(\text{side } i) = \text{Perimeter}(\mathcal{F}).$$

Combining this with (8), one can replace $\int_{\Omega_{\bar{P}}} d\nu$ by the perimeter of $\mathcal{F}$ in the denominator of (7); this completes the proof of Theorem 1.

Remark 5. In [**12**], the authors introduced and investigated dynamical properties of boundary map $f_{\bar{A}}$ defined for an arbitrary multi-parameter $\bar{A} = \{A_1, A_2, \ldots, A_{8g-4}\}$ with all $A_i \in (P_i, Q_i)$ satisfying the so-called 'short cycle property' $f_{\bar{A}}(T_i A_i) = f_{\bar{A}}(T_{i-1} A_i)$. It was proved in [**1**] that $\nu(\Omega_{\bar{A}}) = \nu(\Omega_{\bar{P}})$ and $F_{\bar{A}}$ and $F_{\bar{P}}$ are measure-theoretically isomorphic, which implies that $h_{\nu_{\bar{A}}}(F_{\bar{A}}) = h_{\nu_{\bar{P}}}(F_{\bar{P}})$. This allows us to conclude that $\mu_{\bar{A}} = \mu_{\bar{P}}$ and to prove the same formula (4) for the entropy of $f_{\bar{A}}$:

$$h_{\mu_{\bar{A}}}(f_{\bar{A}}) = \frac{\pi^2(4g-4)}{\text{Perimeter}(\mathcal{F})} = \pi \cdot \frac{\text{Area}(\mathcal{F})}{\text{Perimeter}(\mathcal{F})} = h_{\mu_{\bar{P}}}(f_{\bar{P}}).$$

In other words, the entropy remains unchanged for all boundary maps $f_{\bar{A}}$ defined using a multi-parameter $\bar{A}$ satisfying the short cycle property.

3. *Proof of Theorem 2*

To prove that Theorem 2(i) follows from Theorem 1, we only need to show that for each genus g the perimeter of $\mathcal{F}$ in $\mathcal{T}(S)$ is minimized on the regular polygon.

THEOREM 6. (Isoareal inequality) *Among all hyperbolic polygons with a given area and number of sides, the regular polygon has the smallest perimeter.*

† Thank you to Alena Erchenko for providing this reference.

https://doi.org/10.1017/etds.2021.14 Published online by Cambridge University Press

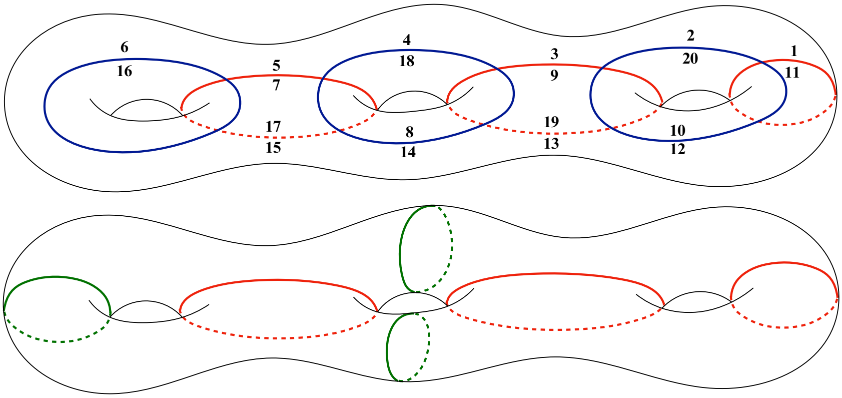

FIGURE 4. Chain of $2g$ geodesics on S forming the sides of $\mathcal{F}$ (top) and decomposition of S into $2g-2$ pairs of pants by $3g-3$ non-intersecting geodesics (bottom) for $g=3$.

Proof. For a hyperbolic n-gon $\mathcal{P}_n$, the inequality

$$\text{Perimeter}(\mathcal{P}_n)^2 \geq 4\, d_n\, \text{Area}(\mathcal{P}_n), \quad d_n = n \tan\left(\frac{\text{Area}(\mathcal{P}_n)}{2n}\right),$$

is given in [**13**, Theorem 1.2(a)], which also states that equality is achieved on a regular polygon. Both isoperimetric and isoareal inequalities follow: $\text{Area}(\mathcal{P}_n)$ and n are constant, so the right-hand side $4d_n\text{Area}(\mathcal{P}_n)$ is constant and thus the perimeter of $\mathcal{F}$ is minimal when $\mathcal{F}$ is a regular polygon. □

In our setting, $\mathcal{F} = \mathcal{P}_n$ with $n = 8g-4$ and $\text{Area}(\mathcal{F}) = 2\pi(2g-2)$ is constant in $\mathcal{T}(S)$, so by Theorem 6 the perimeter is minimized when $\mathcal{F}$ is regular. The expression for the maximum value $H(g)$ in (5) comes directly from (4), with

$$\cosh^{-1}\left(1 + 2\cos\frac{\pi}{4g-2}\right)$$

being the length of a single side of the regular $(8g-4)$-gon. This completes the proof of Theorem 2(i).

To prove Theorem 2(ii), we recall that Fenchel–Nielsen coordinates use a decomposition of S into $2g-2$ pairs of pants by $3g-3$ non-intersecting closed geodesics whose lengths can be manipulated independently (these lengths form $3g-3$ of the $6g-6$ coordinates). We take one of these geodesics to also be a geodesic from the chain described in §1 that corresponds to one entire side of $\mathcal{F}$ (this shared geodesic is on the far right in both parts of Figure 4). Since the length of this side (one of the Fenchel–Nielsen coordinates) can be made arbitrarily large, the perimeter of $\mathcal{F}$ can also be made arbitrarily large, which by (4) means that $h_{\mu_{\bar{P}}}(f_{\bar{P}})$ can be made arbitrarily small.

Using the continuity of the Fenchel–Nielsen coordinates, if $\Gamma \to \Gamma'$ in $\mathcal{T}(S)$, then, by the Fenchel–Nielsen theorem, $\Gamma = h \circ \Gamma' \circ h^{-1}$ for some orientation-preserving homeomorphism $h : \bar{\mathbb{D}} \to \bar{\mathbb{D}}$, and $h|_{\mathbb{S}} \to \text{Id}$ as circle homeomorphisms, that is, $d(h(x), x) \to 0$ for all $x \in \mathbb{S}$. Therefore, for the endpoints of the geodesics $P_i Q_{i+1}$ containing the sides of the fundamental polygon $\mathcal{F}$ and the geodesics $P_i' Q_{i+1}'$ containing the sides of the

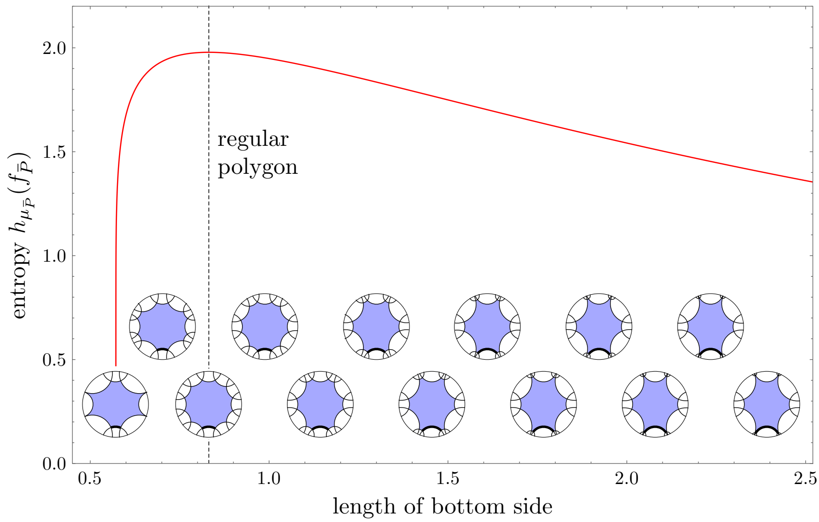

FIGURE 5. Entropy as a function of a single Fenchel–Nielsen coordinate for $g = 2$.

fundamental polygon $\mathcal{F}'$, we have $P_i \to P'_i$ and $Q_{i+1} \to Q'_{i+1}$. It follows that the vertices of $\mathcal{F}$ will tend to the vertices of $\mathcal{F}'$, and hence Perimeter($\mathcal{F}$) $\to$ Perimeter($\mathcal{F}'$), that is, the perimeter of $\mathcal{F}$ varies continuously within the Teichmüller space $\mathcal{T}(S)$. From Theorem 1 we conclude the continuity of the entropy $h_{\mu_{\bar{P}}}(f_{\bar{P}})$ within $\mathcal{T}(S)$. By the intermediate value theorem, $h_{\mu_{\bar{P}}}(f_{\bar{P}})$ must take on all values between 0 and its maximum.

For genus 2, the techniques of Maskit (see Appendix A) allow us to accurately draw the fundamental polygon $\mathcal{F}$ for any values of the Fenchel–Nielsen coordinates. Figure 5 shows how the entropy changes as the single Fenchel–Nielsen coordinate representing the length of the bottom side of $\mathcal{F}$ is varied.

4. *Topological entropy*

The notion of topological entropy was originally introduced for continuous maps acting on compact metric spaces. As explained in [15], Bowen's definition can also be applied to piecewise continuous, piecewise monotone maps on an interval. The theory naturally extends to maps of the circle, where monotonicity is understood to mean local monotonicity.

The map $f_{\bar{P}}$ is Markov with respect to the partition $\{I_1, \ldots, I_{16g-8}\}$ given by

$$I_{2i-1} := [P_i, Q_i), \quad I_{2i} := [Q_i, P_{i+1}), \quad i = 1, \ldots, 8g-4 \tag{9}$$

(see [3, Theorem 6.1]). The associated transition matrix M has entries

$$m_{ij} = \begin{cases} 1 & \text{if } f_{\bar{P}}(I_i) \supset I_j, \\ 0 & \text{otherwise,} \end{cases}$$

and the topological entropy of $f_{\bar{P}}$ is

$$h_{\text{top}}(f_{\bar{P}}) = \log |\lambda_{\max}|,$$

https://doi.org/10.1017/etds.2021.14 Published online by Cambridge University Press

where $|\lambda_{\max}|$ is the spectral radius (that is, the eigenvalue with largest absolute value) of M (see, for example, [11, Proposition 3.2.5]).

In some situations the Lebesgue measure μ will satisfy $h_\mu(f) = h_{\text{top}}(f)$, but the boundary map $f_{\bar{P}} : \mathbb{S} \to \mathbb{S}$ provides an example where the smooth invariant measure $\mu_{\bar{P}}$ is not a measure of maximum entropy (since $f_{\bar{P}}$ is Markov, the measure of maximal entropy is the Parry measure).

It is a direct calculation that $\lambda = 4g - 3 + \sqrt{(4g-3)^2 - 1}$ is an eigenvalue of M with corresponding eigenvector

$$v = (1,\ \lambda{-}1,\ 1,\ \lambda{-}1, \ldots,\ 1,\ \lambda{-}1).$$

This shows that the topological entropy satisfies

$$h_{\text{top}}(f_{\bar{P}}) \geq \log\left(4g - 3 + \sqrt{(4g-3)^2 - 1}\right), \tag{10}$$

which is used in the proof of Corollary 7 below.

We should point out that as we move in the Teichmüller space $\mathcal{T}(S)$, by the Fenchel–Nielsen theorem mentioned in the Introduction, the partition (9) of $\mathbb{S}$ into $16g - 8$ intervals remains Markov with the same transition matrix M, therefore $h_{\text{top}}(f_{\bar{P}})$ does not change.

COROLLARY 7. *The measure-theoretic entropy of $f_{\bar{P}}$ with respect to its smooth invariant measure $\mu_{\bar{P}}$ is strictly less than the topological entropy of $f_{\bar{P}}$.*

Proof. From (5), we have that $H(g) = h_{\mu_{\bar{P}}^{\text{reg}}}(f_{\bar{P}}^{\text{reg}})$, computed in Theorem 2(i), is an increasing function of g, and we can calculate

$$\lim_{g\to\infty} H(g) = \lim_{g\to\infty} \frac{\pi^2(4g-4)}{(8g{-}4)\cosh^{-1}(1{+}2\cos(\pi/(4g-2)))} = \frac{\pi^2}{2\cosh^{-1}(3)}.$$

Since $H(g)$ is increasing, its value for any g is less than or equal to this limit. The function

$$\log\left(4g - 3 + \sqrt{(4g-3)^2 - 1}\right)$$

is also increasing, so, by (10), for any $g \geq 3$ we have

$$h_{\text{top}}(f_{\bar{P}}) \geq \log(9 + 4\sqrt{5}) \approx 2.8872$$

and, therefore,

$$h_{\mu_{\bar{P}}}(f_{\bar{P}}) \ \leq\ \frac{\pi^2}{2\cosh^{-1}(3)} \ <\ 2.8\ <\ \log(9 + 4\sqrt{5})\ \leq\ h_{\text{top}}(f_{\bar{P}}).$$

The case $g = 2$ is checked separately:

$$h_{\mu_{\bar{P}}}(f_{\bar{P}}) = \frac{\pi^2}{3\cosh^{-1}(1+\sqrt{3})} \approx 1.9784, \quad h_{\text{top}}(f_{\bar{P}}) \geq \log(5 + 2\sqrt{6}) \approx 2.2924.$$

This completes the proof of the Corollary 7. □

Remark 8. In [2] we prove that $4g-3+\sqrt{(4g-3)^2-1}$ is the maximal eigenvalue of M, thus making (10) an equality and obtaining the exact formula for $h_{\text{top}}(f_{\bar{P}})$. For Corollary 7, however, the inequality is sufficient.

Acknowledgements. The second author was partially supported by NSF grant DMS 1602409. The third author was partially supported by a Simons Foundation Collaboration Grant. The authors would like to thank the Institute of Mathematics of the Polish Academy of Sciences (IMPAN) for its hospitality. We would also like to thank the anonymous referee for careful reading and, in particular, for pointing out the correct constant relating dm and $d\omega$ in §2.

A. *Appendix. Computational tools for genus 2*

The polygon in Figure 2 and the details of Figure 3 were produced using the generators of Γ in terms of the Fenchel–Nielsen coordinates $(\alpha, \beta, \gamma, \sigma, \tau, \rho)$ for $g=2$ introduced by Maskit [14]. In case they will be useful for others, we provide below the relevant information for doing numerical experiments in $\mathcal{T}(S)$ for genus 2.

Maskit uses the six parameters above along with

$$\mu = \cosh^{-1}\big(\coth\beta\cosh\sigma\cosh\tau + \sinh\sigma\sinh\tau\big),$$

$$\delta = \coth^{-1}\left(\frac{\cosh\gamma\cosh\mu - \coth\alpha\sinh\gamma\sinh\mu - \sinh\sigma\sinh\rho}{\cosh\sigma\cosh\rho}\right)$$

to define matrices $\widetilde{A}, \widetilde{B}, \widetilde{C}, \widetilde{D}$ acting on the half-plane. Setting $A = \frac{1}{2}\left(\begin{smallmatrix} i & 1 \\ 1 & i\end{smallmatrix}\right)\widetilde{A}\left(\begin{smallmatrix} -i & 1 \\ 1 & -i\end{smallmatrix}\right)$, etc., we get the following matrices acting on the unit disk:

$$A = \frac{\sinh\alpha}{\sinh\mu}\begin{pmatrix} \coth\alpha\sinh\mu + i & -i\cosh\mu \\ i\cosh\mu & \coth\alpha\sinh\mu - i \end{pmatrix},$$

$$B = \frac{\sinh\beta}{\cosh\tau}\begin{pmatrix} \cosh\tau\coth\beta + i\sinh\sigma & \cosh\sigma + i\sinh\tau \\ \cosh\sigma - i\sinh\tau & \cosh\tau\coth\beta - i\sinh\sigma \end{pmatrix},$$

$$C = \begin{pmatrix} \cosh\gamma & i\sinh\gamma \\ -i\sinh\gamma & \cosh\gamma \end{pmatrix},$$

$$D = \frac{\sinh\delta}{\cosh\rho}\begin{pmatrix} \cosh\rho\coth\delta - i\sinh(\gamma+\sigma) & -\cosh(\gamma+\sigma) - i\sinh\rho \\ -\cosh(\gamma+\sigma) + i\sinh\rho & \cosh\rho\coth\delta + i\sinh(\gamma+\sigma) \end{pmatrix}.$$

Let S_i be the transformation for which P_i is the repelling fixed point and Q_{i+1} is the attracting fixed point. That is, the oriented axis of S_i contains side i. We have

$$\begin{aligned} &S_1 = C^{-1}D^{-1}C, && S_2 = AC, && S_3 = ABDA^{-1}, && S_4 = A^{-1}, \\ &S_5 = D^{-1}B^{-1}, && S_6 = CA, && S_7 = D, && S_8 = DA^{-1}C^{-1}D^{-1}, \\ &S_9 = B^{-1}D^{-1}, && S_{10} = B^{-1}AB, && S_{11} = C^{-1}DCB, && S_{12} = C^{-1}B^{-1}A^{-1}B. \end{aligned}$$

https://doi.org/10.1017/etds.2021.14 Published online by Cambridge University Press

The side-pairing transformations are

$$T_1 = C, \quad T_2 = C^{-1}DC, \quad T_3 = A^{-1}, \quad T_4 = B^{-1},$$
$$T_5 = A, \quad T_6 = D, \quad T_7 = C^{-1}, \quad T_8 = D^{-1},$$
$$T_9 = B^{-1}AB, \quad T_{10} = B, \quad T_{11} = B^{-1}A^{-1}B, \quad T_{12} = C^{-1}D^{-1}C,$$

and the defining relation

$$ABDA^{-1}C^{-1}D^{-1}CB^{-1} = \mathrm{Id}$$

from [14] is equivalent to [12, Equation 1.5] with $g = 2$. The regular 12-gon corresponds to values

$$\alpha = \tfrac{1}{2}\operatorname{arccosh}(1+\sqrt{3}), \quad \beta = \gamma = 2\alpha, \quad \sigma = \tau = \rho = 0$$

for Maskit's Fenchel–Nielsen coordinates.

References

[1] A. Abrams and S. Katok. Adler and Flatto revisited: cross-sections for geodesic flow on compact surfaces of constant negative curvature. *Studia Math.* **246** (2019), 167–202.

[2] A. Abrams, S. Katok and I. Ugarcovici. Rigidity of topological entropy of boundary maps associated to Fuchsian groups, *Preprint*, 2021, arxiv.org/abs/2101.10271.

[3] R. Adler and L. Flatto. Geodesic flows, interval maps, and symbolic dynamics. *Bull. Amer. Math. Soc.* **25**(2) (1991), 229–334.

[4] J. Birman and C. Series. Dehn's algorithm revisited, with applications to simple curves on surfaces. *Combinatorial Group Theory and Topology (AM-111)*. Princeton University Press, Princeton, NJ, 1987, pp. 451–478.

[5] F. Bonahon. The geometry of Teichmüller space via geodesic currents. *Invent. Math.* **92** (1988), 139–162.

[6] R. Bowen and C. Series. Markov maps associated with Fuchsian groups. *Inst. Hautes Études Sci. Publ. Math.* **50** (1979), 153–170.

[7] W. Fenchel and J. Nielsen. *Discontinuous Groups of Isometries in the Hyperbolic Plane (de Gruyter Studies in Mathematics, 29).* Ed. A. L. Schmidt. Walter de Gruyter & Co., Berlin, 2003.

[8] G. Forni and C. Matheus. Introduction to Teichmüller theory and its applications to dynamics of interval exchange transformations, flows on surfaces and billiards. *J. Mod. Dyn.* **8** (2013), 271–436.

[9] L. Funar. *Lecture Notes for the Summer School 'Géométries à courbure négative ou nulle, groupes discrets et rigidités'*. Institut Fourier, Université de Grenoble, June–July 2004.

[10] E. Hopf. Fuchsian groups and ergodic theory. *Trans. Amer. Math. Soc.* **39**(2) (1936), 299–314.

[11] A. Katok and B. Hasselblatt. *Introduction to the Modern Theory of Dynamical Systems*. Cambridge University Press, Cambridge, 1995.

[12] S. Katok and I. Ugarcovici. Structure of attractors for boundary maps associated to Fuchsian groups. *Geom. Dedicata* **191** (2017), 171–198. Errata: **198** (2019), 189–191.

[13] H.-T. Ku, M.-C. Ku and X.-M. Zhang. Isoperimetric inequalities on surfaces of constant curvature. *Canad. J. Math.* **49** (1997), 1162–1187.

[14] B. Maskit. New parameters for Fuchsian groups of genus 2. *Proc. Amer. Math. Soc.* **127** (1999), 3643–3652.

[15] M. Misiurewicz and K. Ziemian. Horseshoes and entropy for piecewise continuous piecewise monotone maps. *From Phase Transitions to Chaos*. World Scientific Publishing, River Edge, NJ, 1992, pp. 489–500.

[16] P. Schmutz Schaller. Teichmüller space and fundamental domains of Fuchsian groups. *Enseign. Math.* **45** (1999), 169–187.

[17] D. Sullivan. The density at infinity of a discrete group of hyperbolic motions. *Inst. Hautes Études Sci. Publ. Math.* **50** (1979), 171–202.

[18] W. P. Thurston. *Three-Dimensional Geometry and Topology*. Princeton University Press, Princeton, NJ, 1997.

[19] B. Weiss. On the work of Roy Adler in ergodic theory and dynamical systems. *Symbolic Dynamics and its Applications (New Haven, CT, 1991) (Contemporary Mathematics,* 135*)*. American Mathematical Society, Providence, RI, 1992, pp. 19–32.

[20] H. Zieschang, E. Vogt and H. D. Coldewey. *Surfaces and Planar Discontinuous Groups (Lecture Notes in Mathematics,* 835*)*. Springer, Berlin, 1980.

https://doi.org/10.1017/etds.2021.14 Published online by Cambridge University Press